Journal of the Optical Society of America B
OPTICAL PHYSICS

# Broadband laser-driven electromagnetically induced transparency in three-level systems with a double Fano continuum

Doan Quoc Khoa,[1,2,*] Nguyen Ba Duc,[3] Thai Doan Thanh,[4] Ho Quang Quy,[5] Cao Long Van,[6] and Wiesław Leoński[6]

[1]Division of Computational Physics, Institute for Computational Science, Ton Duc Thang University, Ho Chi Minh City, Vietnam
[2]Faculty of Electrical and Electronics Engineering, Ton Duc Thang University, Ho Chi Minh City, Vietnam
[3]Tan Trao University, Tuyen Quang, Vietnam
[4]Food Industry University of HCM City, Ho Chi Minh City, Vietnam
[5]Faculty of Electric Technology and Electronics, Food Industry University of HCM City, Ho Chi Minh City, Vietnam
[6]Quantum Optics and Engineering Division, Institute of Physics, University of Zielona Góra, Prof. A. Szafrana 4a, 65-516 Zielona Góra, Poland
*Corresponding author: doanquockhoa@tdt.edu.vn

Received 20 February 2018; revised 24 April 2018; accepted 5 May 2018; posted 9 May 2018 (Doc. ID 324553); published 6 June 2018

**We discuss the electromagnetically induced transparency (EIT) phenomenon for a model in which a structured continuum is described by a so-called double Fano structure; instead of one autoionizing (AI) state, two such states are embedded in a flat continuum. Such a Fano structure is the upper level of a $\Lambda$-like three-level system and is coupled to two lower ones by an external laser field involving $\delta$-correlated, Gaussian, Markov process (white noise), simulating realistic conditions of the experiment. For such a system we derived and solved a set of coupled stochastic integrodifferential equations in the stationary regime, obtaining exact formulas determining the electric susceptibility of the system. Dispersion and absorption spectra of the medium susceptibility were calculated and compared with those already discussed in the literature. We have shown that the presence of an additional AI level considerably changes the structure of transparency windows and how noisy excitation influences the EIT processes.** 

***OCIS codes:*** (000.5490) Probability theory, stochastic processes, and statistics; (270.1670) Coherent optical effects; (270.2500) Fluctuations, relaxations, and noise.

https://doi.org/10.1364/JOSAB.35.001536

## 1. INTRODUCTION

One of the basic axioms of quantum mechanics is the superposition principle, which leads to quantum interference, the source of numerous counterintuitive but very fascinating quantum effects. One of the phenomena in which such interference plays a crucial role is electromagnetically induced transparency (EIT). In this phenomenon, a strong driving field interacts with the medium in such a way that its optical properties are modified. As a result, the incident weak probe beam will pass through the medium without being absorbed. It should be emphasized that EIT is a subject of intensive studies discussed in a growing number of papers (for examples, see [1–10] and the references quoted therein).

One can simply explain the EIT effect by taking one of the basic configurations considered in the literature with three discrete atomic levels, namely, Λ-type configuration. Such a system consists of two lower bound states and one upper excited one and initially is not transparent for an incoming resonant probing laser beam, but becomes transparent under the influence of another stronger control laser beam. The coherent interaction of the atomic system with two laser beams leads to the creation of a so-called dark state, being a superposition of two lower states that do not couple with the upper one. The destructive interference between two possible paths of excitation appears, and then the atomic system does not absorb the incoming radiation—the medium becomes transparent for the probing beam. In consequence, the dispersive properties of the considered system are controlled by the intensity of the control laser beam. For such a situation, one can change the group velocity of the probing pulse, with a possibility of completely stopping it for the storage of information when the control pulse is excluded. In the experiment of the Haus group in 1999 [9] for the gas of sodium atoms cooled to the temperature of a few nanokelvin, the probing pulse was slowed to the velocity of 17 m/s. In 2001, this group was able to complete stop it for the period of time 1.5 μs [11]. Thanks to this big progress in

experimental techniques, such time of storage of the light pulse has been enlarged to more than 1 s [12]. As the light slowing the transition time through the medium becomes longer, so the interaction time of light with the medium increases. Therefore, it has also been observed [9] that such a medium is characterized by extremely large optical nonlinearities (giant Kerr nonlinearities), which has been predicted by Schmidt and Imamoğlu [13]. In Ref. [9], the Kerr refractive index has been calculated, showing that it can be a million times bigger than that in cold cesium atoms and approximately 1013 times larger than traditional ones. Such a medium can be treated as giving new possibilities in experimental investigation in the field of quantum optics [14]. The media described by giant Kerr nonlinearities are very interesting from the point of view of various applications, in particular those related to quantum information theory. For example, Imoto *et al.* [15] already proposed the scheme of measuring the number of photons that does not destroy their state (quantum nondemolition measurement). Moreover, various maximally entangled states can be generated in Kerr-like "couplers" (multimode systems involving such huge nonlinearities that interact with each other and whose evolution is governed by the same effective Hamiltonians as usual optical couplers) [16–18] in the regime of *nonlinear quantum scissors* [16].

Other quantum interference effects that have an even longer history and through a long time period have been a central subject for quantum optical study; such studies relate to autoionization (AI) processes, where the possible quantum interference paths connect both the discrete and continuum levels involved in the considered system. AI systems have been studied in a large number of publications since 1961, when Fano published his classical paper [19]. Fano diagonalization based on the mixing of ionizing levels with the continuum gives us the nontrivial structure of the latter. Models containing several discrete levels lying above continuum threshold (AI levels) have been the subject of numerous papers in atom-laser physics (see [19–35] and the references quoted therein). These models are usually referred to as Fano systems and/or Fano-like systems. They are also studied in more realistic models, where the driven electromagnetic field involved a white-noise component, for both the single [36] and double Fano profile [37]. They appeared also in other physical situations, for example, in nanophysics, metamaterials [38], in the description of quantum dots [39–41], and in considering noninteracting waveguide arrays [42]. Several review papers have been devoted to Fano-like systems [43,44]. They are involved also in the papers considering propagation of electromagnetic waves in atomic media [45–47].

We know that a real laser is never perfectly monochromatic —its field generally fluctuates in amplitude and phase. Because the microscopic natural world is extremely complex, we model it by classical stochastic processes, which are time-dependent. The dynamical equations, which contain field parameters involved in the considered problem, become stochastic differential equations. Obtaining exact solutions of such stochastic equations is a very difficult task, except for some special cases when, for example, the presence of white noise is assumed. As was shown in Refs. [35,36], such modeling of a laser field with application of stochastic processes can lead to various interesting results. Moreover, models taking into account white noise are interesting by themselves, because they describe electric field amplitude of the multimode laser, operating without any correlation between the modes.

EIT in a model of Λ-like system consisting of a continuum coupled to an AI and two lower bound states has been considered in Ref. [48], where the analytic expressions for the susceptibility for the case of bound-continuum dipole matrix elements were modeled according to Fano theory [19]. Then, in Ref. [48], the shapes of transparency windows depending on the amplitude of the control field were considered. In our previous work [49], we extended the formalism introduced there to the same Λ-like system, in which instead of the strictly monochromatic control laser field, that perturbed by so-called white noise was considered. It was shown there that the set of coupled stochastic integrodifferential equations describing the problem can be solved exactly. Obtained spectra of real and imaginary parts of the medium susceptibility were calculated analytically and compared to the results obtained in Ref. [48].

The model considered in Ref. [48] has been extended to the case of double Fano structures [50], in which instead of one AI state, we have two of them embedded in one continuum [51]. We have known that the appearance of an additional EIT window is due to the presence of the second AI level. Furthermore, the characteristics of this window can be manipulated by changes of the parameters describing AI levels and their interaction with external fields. In this paper, we use the same method discussed in Ref. [49] and the model considered in Ref. [51], in which a fluctuating control field is modeled by white noise. In consequence, we solve exactly the set of coupled stochastic integrodifferential equations describing the behavior of our system. The spectra of dispersion and absorption parts of the electric susceptibility are calculated and compared with the results previously discussed in the literature. We show that for the cases when the control field fluctuates, the structure of the EIT windows changes dramatically.

Our paper is organized as follows: In the next section, some details of our model are described, and the set of equations for atomic operators involved in the problem is derived. In the third part, our results are presented and discussed. The last section contains conclusions.

## 2. MODEL OF THE Λ-LIKE THREE-LEVEL SYSTEM WITH DOUBLE FANO STRUCTURE

In this paper, we consider the Λ-like system that is shown in Fig. 1. This system includes two lower states, $|b\rangle$ and $|c\rangle$, the flat continuum $|E\rangle$, and two AI states, $|a_1\rangle$ and $|a_2\rangle$, which are coupled with the continuum by two couplings, $U_1$ and $U_2$, respectively [50–53]. The continuum and the AI states are coupled with discrete levels $|c\rangle$ and $|b\rangle$ by strong control and weak probe fields. They are described by amplitudes $\varepsilon_d$ and $\varepsilon_p$, and frequencies $\omega_d$ and $\omega_p$, respectively. As usual in the papers concerning AI phenomena, for simplicity the frequency $\omega_d$ is supposed not large enough to allow for the transition from the state $|b\rangle$ to the continuum, and level shifts are ignored because of nonresonant couplings that can be taken into account by redefining involved detuning. The appearance

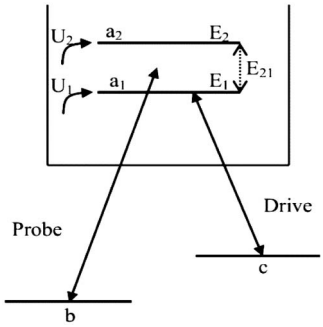


**Fig. 1.** Scheme of the levels and couplings.

of the AI states may be alternatively taken into account by a prediagonalization procedure that leads to a dressed continuum $|E\rangle$ with a modified density of states [19].

Similarly, as in Ref. [49], we also suppose that the amplitude of the driving field is

$$\varepsilon_d = \varepsilon_{0d} + \varepsilon(t), \tag{1}$$

in which $\varepsilon_{0d}$ is a deterministic coherent part of the driving field and $\varepsilon(t)$ is characterized by a Gaussian, Markov, and steady process (white noise):

$$\langle\langle \varepsilon(t)\varepsilon^*(t')\rangle\rangle = a_0\delta(t-t'). \tag{2}$$

The $\langle\langle\rangle\rangle$ in Eq. (2) is the notation of averaging over the ensemble of realizations of the process $\varepsilon(t)$. By using the Liouville–von Neumann equation in the rotating wave approximation (RWA) to depict the evolution of the atomic system and applying the formalism of Fano diagonalization, we obtain the set of the following equations for the density matrix $\rho(z,t)$:

$$\begin{aligned} i\hbar\dot{\rho}_{Eb} &= (E - E_b - \hbar\omega_p)\rho_{Eb} - \frac{1}{2}(E|d|b\rangle\varepsilon_p \\ &\quad - \frac{1}{2}(E|d|c\rangle(\varepsilon_{0d} + \varepsilon(t))\rho_{cb}, \\ i\hbar\dot{\rho}_{cb} &= (E_c + \hbar\omega_d - E_b - \hbar\omega_p - i\hbar\gamma_{cb})\rho_{cb} \\ &\quad - \frac{1}{2}(\varepsilon_{0d} + \varepsilon(t))^* \int \langle c|d|E\rangle\rho_{Eb}\mathrm{d}E, \end{aligned} \tag{3}$$

where $d$ is the electric dipole moment of the atomic system, $\gamma_{cb}$ denotes a phenomenological relaxation rate for the coherence $\rho_{cb}$, and $\rho_{Eb} = (E|\rho|b)$.

Thus, from Eqs. (1) and (2), we can see that Eq. (3) corresponds to the stochastic differential equation of the form

$$\frac{dQ}{dt} = \{M_1 + x(t)M_2 + x*(t)M_3\}Q + M_4. \tag{4}$$

Here, $Q$ denotes a vector function of time, whereas $M_i$, $i = 1,2,3,4$ are constant matrices. Next, we apply the well-known multiplicative stochastic process theory result (see, for example, Ref. [36]); we assume that the function $\langle\langle Q\rangle\rangle$ satisfies the nonstochastic equation of the form

$$\frac{d\langle\langle Q\rangle\rangle}{dt} = [M_1 + a_0\{M_2, M_3\}/2]\langle\langle Q\rangle\rangle + M_4, \tag{5}$$

with $\{M_2, M_3\}$ denoting the anticommutator of $M_2$ and $M_3$.

From there, the set of equations for stochastic averages of the variables are derived (for convenience, $\langle\langle\rangle\rangle$ have been dropped):

$$\begin{aligned} i\hbar\dot{\rho}_{Eb} &= [(E - E_b - \hbar\omega_p) + \frac{a_0}{8}(E|d|c\rangle\langle c|d|E)]\rho_{Eb} \\ &\quad - \frac{1}{2}(E|d|b\rangle\varepsilon_p - \frac{1}{2}(E|d|c\rangle b_0\rho_{cb}, \\ i\hbar\dot{\rho}_{cb} &= [(E_c + \hbar\omega_d - E_b - \hbar\omega_p - i\hbar\gamma_{cb}) \\ &\quad + \frac{a_0}{8}\langle c|d|E)(E|d|c\rangle]\rho_{cb} - \frac{1}{2}b_0^*\int \langle c|d|E)\rho_{Eb}\mathrm{d}E, \end{aligned} \tag{6}$$

where $b_0 = |\varepsilon_{0d}|$. We can get the density matrix elements necessary for determination of the medium susceptibility by using the solutions of Eq. (6).

## 3. MEDIUM SUSCEPTIBILITY SPECTRUM

We can obtain the medium susceptibility spectrum $\chi(\omega_p)$ from the density matrix elements by applying the following relation:

$$P^+(\omega_p) = N\int d_{bE}\rho_{Eb}\mathrm{d}E = \varepsilon_0\varepsilon_p\chi(\omega_p). \tag{7}$$

Here $N$ denotes the atom density, and $\varepsilon_0$ is the vacuum electric permittivity. From there, $\chi(\omega_p)$ has the form

$$\chi(\omega_p) = -\frac{N}{\varepsilon_0}\left(K_{bb} + \frac{\frac{1}{4}b_0^2K'_{bc}K_{cb}}{E_b + \hbar\omega_p - E_c - \hbar\omega_d - i\hbar\gamma_{cb} - \frac{1}{4}b_0^2K_{cc}}\right), \tag{8}$$

where the functions $K_{ij}(\omega_p)$ and $K'_{ij}(\omega_p)$, $i,j = b,c$, have the following form:

$$K_{ij}(\omega_p) = \lim_{\eta\to 0^+}\int \frac{\langle i|d|E)(E|d|j\rangle}{E_b + \hbar\omega_p - E - \frac{a_0}{8}\langle c|d|E)(E|d|c\rangle + i\eta}\mathrm{d}E, \tag{9}$$

$$\begin{aligned} K'_{ij}(\omega_p) &= \lim_{\eta\to 0^+}\int \frac{\langle i|d|E)(E|d|j\rangle}{E_b + \hbar\omega_p - E - \frac{a_0}{8}\langle c|d|E)(E|d|c\rangle + i\eta} \\ &\quad \times \frac{1}{1 + \frac{a_0}{8}\frac{\langle c|d|E)(E|d|c\rangle}{E_c + \hbar\omega_d - E_b - \hbar\omega_p - i\hbar\gamma_{cb} + (1/4)b_0^2K_{cc}}}\mathrm{d}E, \end{aligned} \tag{10}$$

and the limit $\eta \to 0^+$ assures nonnegativity of the imaginary part of susceptibility $\chi$. We model the bound-dressed continuum dipole matrix element the same as in Ref. [51]:

$$\begin{aligned} &\frac{\langle j|d|E)}{\langle j|d|E\rangle} \\ &= \frac{(E - E_1)(E - E_2) + E(q_{1j}\gamma_1 + q_{2j}\gamma_2) - (E_1q_{2j}\gamma_2 + E_2q_{1j}\gamma_1)}{(E - E_1)(E - E_2) - iE(\gamma_1 + \gamma_2) + i(E_1\gamma_2 + E_2\gamma_1)}, \end{aligned} \tag{11}$$

where $\gamma_1 = \pi|\langle a_1|U_1|E\rangle|^2$ and $\gamma_2 = \pi|\langle a_2|U_2|E\rangle|^2$ are AI widths, and as in Ref. [50], we have applied Fano asymmetry parameters $q_{1j}$ and $q_{2j}$, which can be expressed as

$$q_{1j} = \frac{\langle j|d|a_1\rangle}{\pi\langle j|d|E\rangle\langle E|U|a_1\rangle}, q_{2j} = \frac{\langle j|d|a_2\rangle}{\pi\langle j|d|E\rangle\langle E|U|a_2\rangle}, \quad j = b,c. \tag{12}$$

The function inside the integrals holds matrix elements corresponding to the transitions to the structured continuum $|E\rangle$. We should use the formula (11) to get the explicit dependence

of the integrand on the energy because such elements are energy-dependent. Therefore, $K_{ij}(\omega_p)$ and $K'_{ij}(\omega_p)$ can be rewritten as

$$K_{ij}(\omega_p) = \lim_{\eta\to 0^+} D_i D_j \int \frac{F_i(E)F_j(E)}{E_b + \hbar\omega_p - E - \frac{a_0 D_c^2}{8}|F_c(E)|^2 + i\eta}\mathrm{d}E, \tag{13}$$

$$K'_{ij}(\omega_p) = \lim_{\eta\to 0^+} D_i D_j \int \frac{F_i(E)F_j(E)}{E_b + \hbar\omega_p - E - \frac{a_0 D_c^2}{8}|F_c(E)|^2 + i\eta} \times \frac{1}{1 + \frac{a_0 D_c^2}{8}\frac{|F_c(E)|^2}{E_c + \hbar\omega_d - E_b - \hbar\omega_p - i\hbar\gamma_{cb} + (1/4)b_0^2 K_{cc}}}\mathrm{d}E, \tag{14}$$

in which

$$F_i(E) = (Q_i + i)\left(\frac{1}{Q_i + i} + \frac{K_j^+}{E - E_+} + \frac{K_j^-}{E - E_-}\right),$$
$$F_j(E) = (Q_j - i)\left(\frac{1}{Q_j - i} + \frac{(K_k^+)^*}{E - (E_+)^*} + \frac{(K_k^-)^*}{E - (E_-)^*}\right). \tag{15}$$

Appearing here, $E_\pm$ denote the complex roots of the denominator of Eq. (11), and they have the form

$$E_\pm = \frac{E_1 + E_2 \pm K_1}{2} + i\frac{\Gamma \pm K_2}{2}, \tag{16}$$

where

$$K_1 = \frac{1}{\sqrt{2}}\{[(E_{21}^2 - \Gamma^2)^2 + 4E_{21}^2(\gamma_2 - \gamma_1)^2]^{\frac{1}{2}} + \mathrm{E}_{21}^2 - \Gamma^2\}^{\frac{1}{2}},$$
$$K_2 = \frac{1}{\sqrt{2}}\{[(E_{21}^2 - \Gamma^2)^2 + 4E_{21}^2(\gamma_2 - \gamma_1)^2]^{\frac{1}{2}} - \mathrm{E}_{21}^2 + \Gamma^2\}^{\frac{1}{2}}. \tag{17}$$

The parameters $K_j^\pm$ are the complex amplitudes, which are given by the formula as

$$K_j^\pm = \frac{\Gamma}{2}\left(1 \pm \frac{E_{21}L_j + i\Gamma}{K_1 + iK_2}\right), \tag{18}$$

with

$$L_j = \frac{Q_{j21} + i\Gamma_{21}}{Q_j + i}. \tag{19}$$

We have introduced here the separation between two AI levels $E_{21} = E_2 - E_1$, and effective asymmetry parameters $Q_j$, $Q_{j21}$, $\Gamma_{21}$, and AI width $\Gamma$ are given by the following formulas:

$$Q_j = \frac{q_{1j}\gamma_1 + q_{2j}\gamma_2}{\Gamma},$$
$$Q_{j21} = \frac{q_{2j}\gamma_2 - q_{1j}\gamma_1}{\Gamma}, \qquad j = b, c, \tag{20}$$

$$\Gamma = \gamma_1 + \gamma_2, \qquad \Gamma_{21} = \frac{\gamma_2 - \gamma_1}{\Gamma}. \tag{21}$$

Furthermore, the matrix elements of the dipole moment transition $\langle i|d|E\rangle$ and $\langle E|d|j\rangle$ are denoted by $D_i$ and $D_j$, respectively.

If we omit threshold effects, we can extend the integration limits $K_{ij}(\omega_p)$ and $K'_{ij}(\omega_p)$ from minus to plus infinities and obtain the analytical solutions for those parameters. From there, we can derive the electric susceptibility $\chi$.

From the above formulas, we can compute numerically the medium susceptibility $\chi(\omega_p)$ in the stationary regime, which means that the time derivatives appearing in Eq. (6) are equal to zero. We do not present the form of the final solution here because it is very intricate and unreadable. These results will be discussed in a graphical form in the next figures.

We suppose the same values for the parameters depicting an atomic system and its interaction with external fields to compare the results in this paper with those in Refs. [49,51]. Therefore, we put for $\Gamma = 10^{-9}$ a.u., $D_b = 2$ a.u., and $D_c = 3$ a.u. Moreover, the values of the parameter $b_0$ range from $10^{-9}$ to $10^{-6}$ (all parameters used here are in atomic units). In addition, $N = 0.33 \times 10^{12}$ cm$^{-3}$, the asymmetry parameters are of the order of 10–100. $\gamma_{cb}$ is omitted, and detuning $\omega$ has the form $\omega = \omega_p + (E_b - E_1)/\hbar$. Finally, we assume that the parameters describing the AI level decay are identical ($\Gamma_{21} = 0$ and $Q_{j21} = 0$ for $j = b, c$).

The spectra of dispersion (real) and absorption (imaginary) components of the susceptibility for different values of the parameters are shown in Figs. 2–7.

We now discuss two interesting limits: weak and strong fluctuations of the laser field.

For the case of weak fluctuations, if the coherent component of the light dominates over the fluctuations, then we can suppose that the fluctuation component of the field amplitude is zero ($a_0 = 0$), so our results become exactly the same as those from Ref. [51]. Actually, we see that for the case $E_{21} = 0$, we get the same result as for the model with a single AI level discussed by Raczyński *et al.* [48]. Moreover, for the case $E_{21} \to 0$, our result becomes exactly the same as that obtained in Ref. [54]. The dispersion and absorption components of the medium susceptibility without a fluctuations component are shown in Figs. 2 and 3 and have been already discussed in detail in Ref. [51]. Indeed, we see that the model discussed here naturally reduces to that of Bui Dinh *et al.*, when the additional EIT window appears.

Figure 2 shows the dispersion and absorption components of the medium susceptibility for different strengths of control field intensity $b_0$ when the fluctuations part is absent. We can see that changes of $b_0$ can influence the depths and widths of the transparency windows; namely, when the value of $b_0$ increases, the depths of the transparency windows decrease, whereas their widths increase. In addition, the widths of the first windows on the left increase considerably in comparison to those of the second windows on the right. Moreover, the spectral positions of the EIT windows remain unchanged.

In Fig. 3, we show the spectra of real and imaginary components of the medium susceptibility for various values of the separation of energies $E_{21}$ of two AI levels. When $E_{21} = 0$, only an EIT window appears in the spectra, but if $E_{21} \neq 0$, two EIT windows occur in it. The mechanism leading to the transparency window for the weak probe beams appears because quantum interference of the probability amplitudes for these two transition pathways from the ground state to the final state via each of the resonances of AI level ($|a_1\rangle$ or $|a_2\rangle$) with the configuration interaction ($U_1$ or $U_2$),

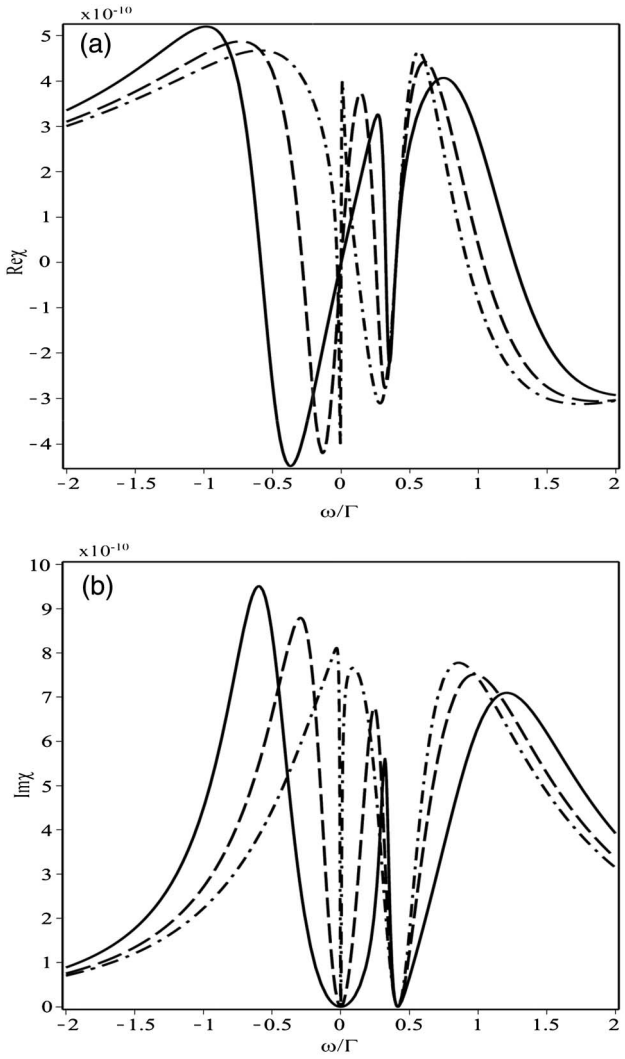


**Fig. 2.** (a) Dispersion and (b) absorption parts of the medium susceptibility as a function of $\omega/\Gamma$. The parameters are $Q_b = Q_c = 10$, $\Gamma = 10^{-9}$ a.u., $E_{21} = 0.8\Gamma$, $a_0 = 0$. Dashed dotted lines, $b_0 = 10^{-7}$ a.u.; dashed lines, $b_0 = 5 \times 10^{-7}$ a.u.; solid lines, $b_0 = 9 \times 10^{-7}$ a.u.

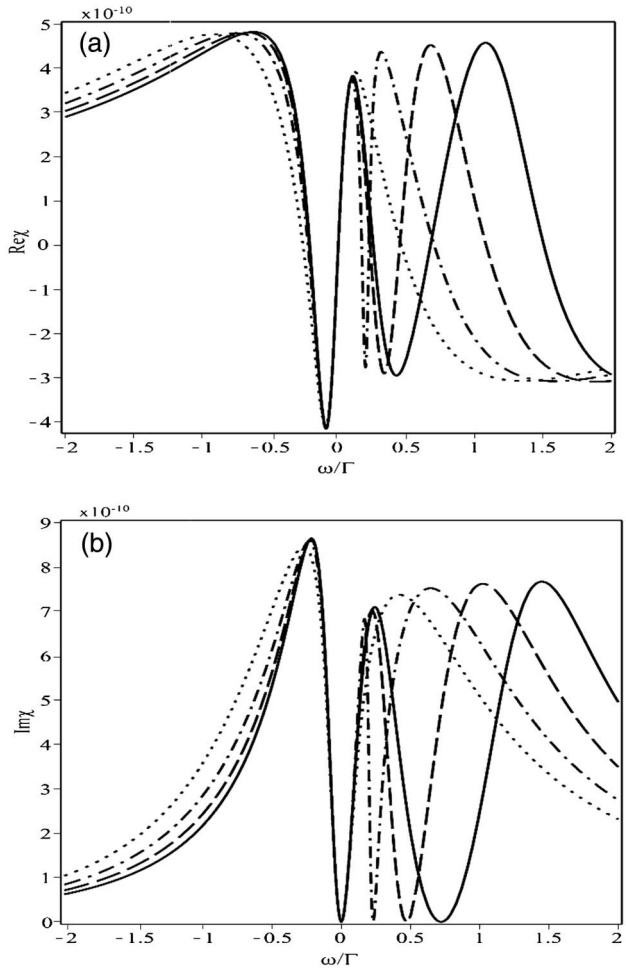


**Fig. 3.** (a) Dispersion and (b) absorption parts of the medium susceptibility as a function of $\omega/\Gamma$. The parameters are $Q_b = Q_c = 10$, $\Gamma = 10^{-9}$ a.u., $b_0 = 4 \times 10^{-7}$ a.u., $a_0 = 0$. Dotted lines, $E_{21} = 0$; dashed dotted lines, $E_{21} = 0.45\Gamma$; dashed lines: $E_{21} = 0.9\Gamma$; solid lines, $E_{21} = 1.35\Gamma$.

respectively, is destroyed. It has been shown that the presence of an arbitrary additional AI level results in new quantum interference phenomena, which can induce an additional EIT window. Thus, a second transparency window originating in the presence of the second AI level has been revealed. We can see that the position of additional window changes according to the energy of the second AI level when values of $E_{21}$ change, and the larger the $E_{21}$, the more distant the second transparency window is from the first one; namely, when the values of $E_{21}$ increase, the distance of the second EIT window from the first window also increases in the same amount of time. This means that increase of the distance of the second window from the first window is proportional to the increase of values of $E_{21}$. Furthermore, when $E_{21}$ increases, the spectral position and width of the first transparency window remain almost unchanged, whereas the width of the spectral of the second transparency window increases. If values of the difference $E_{21}$ are sufficiently large, the second window becomes even broader than the first window.

For the case of strong fluctuations of the laser field, we have now the situation when the coherent component of the strong control field is inconsiderable ($b_0 = 0$) in comparison to the chaotic component. Then the light is pure noise, so we can rewrite $\chi(\omega_p)$ in the form

$$\chi(\omega_p) = -\frac{N}{\varepsilon_0} K_{bb}. \tag{22}$$

Figure 4 shows the real and imaginary components of the medium susceptibility for the cases without the control field or when only the chaotic component of the control field is present. We can see in Fig. 4 that one of two dispersion curves and absorption windows disappears, because in the absence of the control field or when the strong control field fluctuates, the quantum interferences for the appearance of one of the two dispersion curves or EIT windows are weakened. When the chaotic component is present, the slopes of the dispersion curve and absorption profiles drop. In addition, when the chaotic

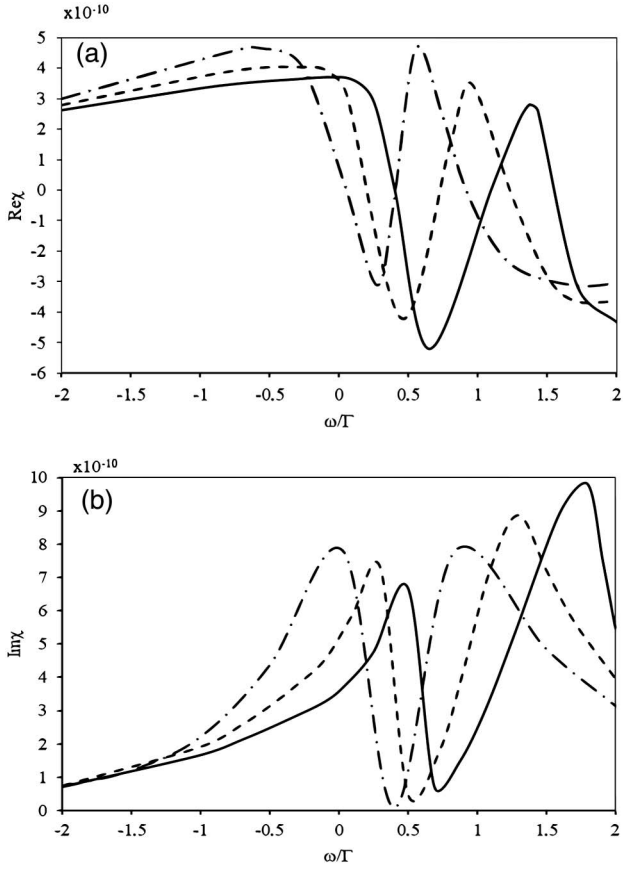


**Fig. 4.** (a) Dispersion and (b) absorption parts of the medium susceptibility as a function of $\omega/\Gamma$. The parameters are $Q_b = Q_c = 10$, $\Gamma = 10^{-9}$a.u., $E_{21} = 0.8\Gamma$, $b_0 = 0$. Dashed dotted lines, $a_0 = 0$; dashed lines, $a_0 = 0.0025\Gamma$; solid lines, $a_0 = 0.005\Gamma$.

component exists, the transparency window shifts to the right; namely, when the fluctuations component increases many times, the transparency window is shifted to the right the same number of times in comparison with the case when the chaotic component is absent. That means a shift in the position of the transparency window is proportional to the increase of the fluctuations component. This effect was discussed by Doan Quoc *et al.* [49] for the case of a single AI level.

However, for the general case, not only the coherence component of the strong control field amplitude exists, but the fluctuating component also plays a significant role. The dispersion and absorption parts of the medium susceptibility for such cases are presented in Figs. 5 and 6. If, additionally, we assume that AI levels are of equal energy ($E_1 = E_2$), our result becomes exactly the same as that obtained by Doan Quoc *et al.* [49]. In addition, for the case $E_{21} \to 0$, we get the same result as for the model with two AI levels of the same energy shown in Ref. [55]. These results have been already discussed in detail in Refs. [49,55]. Indeed, we see that for such a case, the model discussed here reduces to that of Refs. [49,55].

Figure 5 presents the dispersion and absorption parts of the medium susceptibility as functions of $\omega/\Gamma$ for the case when $E_{21} = 0.4\Gamma$ with different values of the fluctuation component. If the chaotic component is absent, our result becomes exactly the same as that obtained in Ref. [51]. When the chaotic component is present, the spectrum contains two transparency windows, but the slope of the dispersion curve and absorption profiles drops. Moreover, the zero point shifts to the right when the chaotic component exists.

In Fig. 6, we show the dispersion and absorption parts of the medium susceptibility as functions of $\omega/\Gamma$ for the case $E_{21} = 0.8\Gamma$ with different values of the fluctuation component when the chaotic part is absent or present. When the chaotic part is absent, our results become also exactly the same as those discussed in Ref. [51]. When the chaotic part is present, we also find that the left peaks of dispersion and left absorption profiles drop faster than others. Moreover, the width of the second transparency window increases and the slope of the second dispersion curves decreases in comparison with the results described in Fig. 5 for the case $E_{21} = 0.4\Gamma$. Furthermore, the transparency window also shifts to the right from the zero frequency.

The weak probe beam, which has group velocity, depends on both the group index, and its changes are related to the derivative of $\mathrm{Re}\chi(\omega_p)$ for the weak probe beam frequency. This fact can be expressed the same as in Ref. [48]:

$$n_g = 1 + \frac{\omega_p}{2}\frac{d}{d\omega_p}\mathrm{Re}\chi(\omega_p). \tag{23}$$

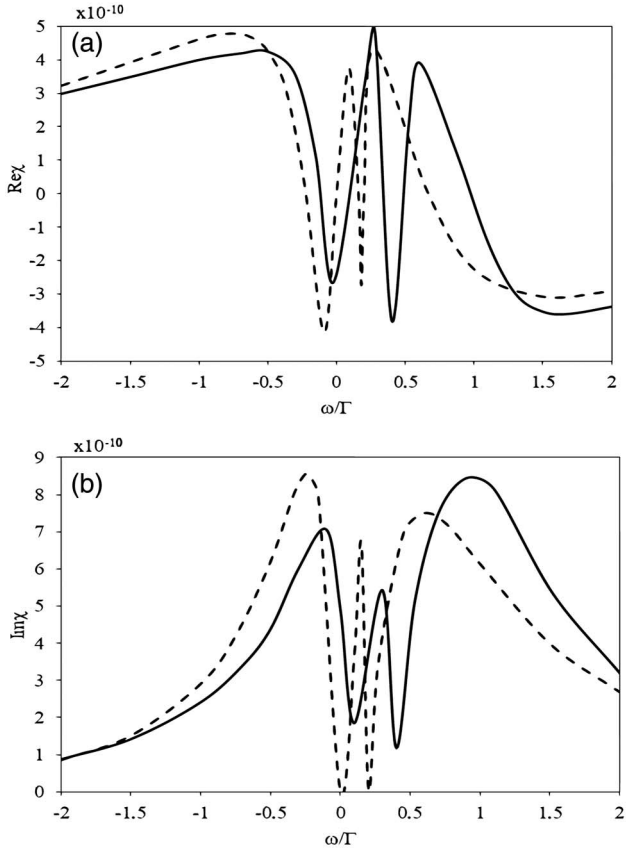


**Fig. 5.** (a) Dispersion and (b) absorption parts of the susceptibility as a function of $\omega/\Gamma$ and the coherent part $b_0 = 4 \times 10^{-7}$a.u., $\Gamma = 10^{-9}$a.u. and $Q_b = Q_c = 10$, $E_{21} = 0.4\Gamma$. Dashed lines, $a_0 = 0$; solid lines, $a_0 = 0.0025\Gamma$.

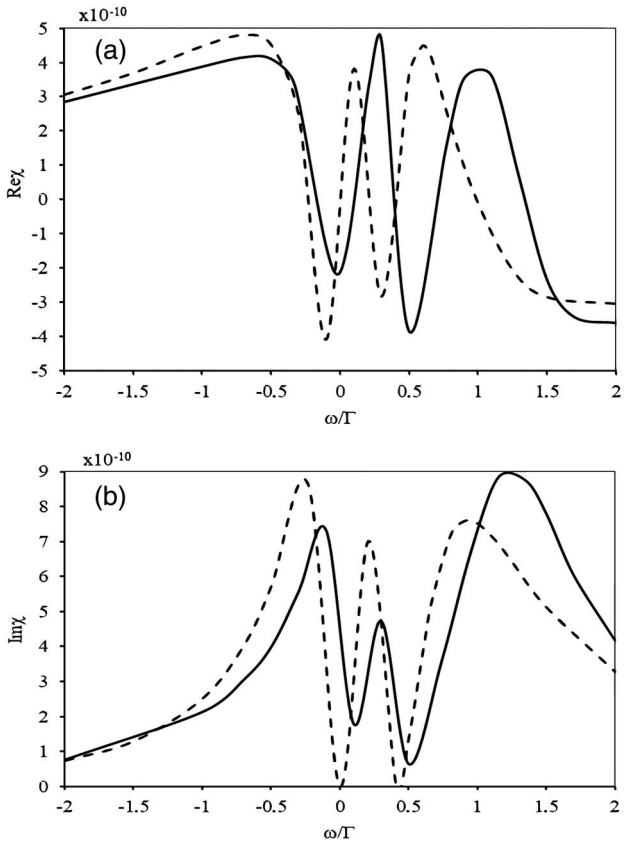


**Fig. 6.** (a) Dispersion and (b) absorption parts of the susceptibility as a function of $\omega/\Gamma$ and the coherent part $b_0 = 4 \times 10^{-7}$a.u., $\Gamma = 10^{-9}$a.u. and $Q_b = Q_c = 10$, $E_{21} = 0.8\Gamma$. Dashed lines, $a_0 = 0$; solid lines, $a_0 = 0.0025\Gamma$.

Then, expression of the group velocity has the following form:

$$v_g = \frac{c}{n_g}, \tag{24}$$

where $c$ is the speed of light in vacuum. Hence, if the slope of the dispersion curves increases, then the group velocity of light decreases.

In Fig. 7, we show in detail the relation between the slope of dispersion curves and the group velocity of light in which the tangent equations corresponding to the curves with $E_{21} = 0.6\Gamma$, $E_{21} = 1.2\Gamma$, and $E_{21} = 1.8\Gamma$ at the coordinates (0.3, 0), (0.6, 0), and (0.9, 0) have the form

$$y_1 = 9.302325580 \times 10^{-9}\omega - 2.790697674 \times 10^{-9}, \tag{25a}$$

$$y_2 = 2.272727273 \times 10^{-9}\omega - 1.363636364 \times 10^{-9}, \tag{25b}$$

$$y_3 = 0.941176470 \times 10^{-9}\omega - 0.847058823 \times 10^{-9}. \tag{25c}$$

We can see that the slope of dispersion curves decreases when the values of $E_{21}$ increase. It follows that the slope of the tangents and the group index increase when the values of $E_{21}$ decrease. Thus, the group velocity of light decreases when the group index increases. From Eq. (25), we can see that the slope

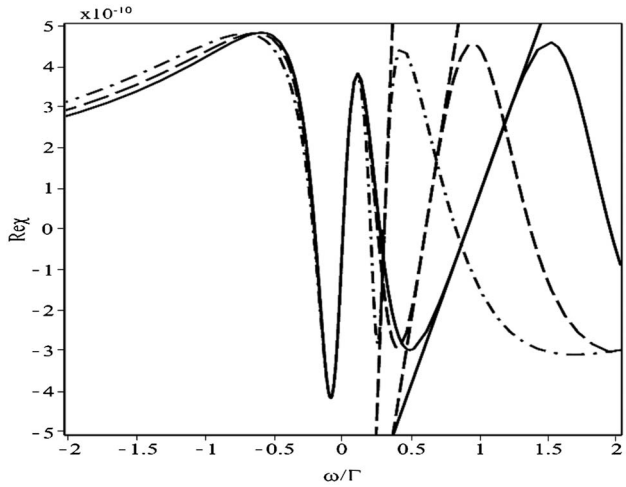


**Fig. 7.** Dispersion parts of the medium susceptibility and their tangents $y_1$, $y_2$, and $y_3$ with the coordinates (0.3, 0), (0.6, 0), and (0.9, 0), respectively. The parameters are $Q_b = Q_c = 10$, $\Gamma = 10^{-9}$a.u., $b_0 = 4 \times 10^{-7}$a.u., $a_0 = 0$. Dashed dotted lines, $E_{21} = 0.6\Gamma$; dashed lines, $E_{21} = 1.2\Gamma$; solid lines, $E_{21} = 1.8\Gamma$.

of Eq. (25a) is 4 times larger than the slope of Eq. (25b) and is approximately 10 times greater than the slope of Eq. (25c). Therefore, the group velocity of light of Eq. (25a) will decrease approximately 4 times and 10 times compared with the group velocity of light in Eqs. (25b) and (25c), respectively.

## 4. SUMMARY

In the present study, we have presented the atomic model of a Λ-like system that is the so-called double Fano continuum, in which instead of one AI level, we have two AI levels embedded in the flat continuum [51]. As in Ref. [36], we also suppose that the laser light of the strong control fields applied in this system is decomposed into two parts: a deterministic component (coherent component) and a randomly fluctuating chaotic part (white noise). By solving a set of stochastic integrodifferential equations involved in the problem, we derived a system for the steady solution for the medium susceptibility. Next, the exact expressions of the dispersion and absorption spectra of the electric susceptibility were obtained, and we compared them with those obtained in Ref. [51]. The EIT phenomenon also exists for the Λ-like systems considered in the present work. In addition, not only the position but also the width of the transparency window changes dramatically in comparison with the case when the noise of the strong control field is absent.

Similar to the case discussed in Ref. [49], because the amplitudes of the real laser light, which in experimental setups always contain some fluctuating part, so we have confidence our model is more realistic than that described by Bui Dinh *et al.* [51].

**Funding.** Vietnam National Foundation for Science and Technology Development (NAFOSTED) (103.03-2017.28).

## REFERENCES


1. A. Imamoğlu and S. E. Harris, "Laser without inversion: interference of dressed lifetime-broadened states," Opt. Lett. **14**, 1344–1346 (1989).
2. S. E. Harris, J. E. Field, and A. Imamoğlu, "Nonlinear optical processes using electromagnetically induced transparency," Phys. Rev. Lett. **64**, 1107–1110 (1990).
3. J. E. Field, K. H. Hahn, and S. E. Harris, "Observation of electromagnetically induced transparency in collisionally broadened lead vapor," Phys. Rev. Lett. **67**, 3062–3065 (1991).
4. K. J. Boller, A. Imamoğlu, and S. E. Harris, "Observation of electromagnetically induced transparency," Phys. Rev. Lett. **66**, 2593–2596 (1991).
5. A. Imamoğlu, J. E. Field, and S. E. Harris, "Lasers without inversion: a closed lifetime broadened system," Phys. Rev. Lett. **66**, 1154–1156 (1991).
6. K. Kowalski, V. Cao Long, H. Nguyen Viet, S. Gateva, M. Głódź, and J. Szonert, "Simultaneous coupling of three hfs components in a cascade scheme of EIT in cold 85Rb atoms," J. Non-Cryst. Solids **355**, 1295–1301 (2009).
7. A. Żaba, V. Cao Long, M. Głódź, E. Paul-Kwiek, K. Kowalski, J. Szonert, D. Woźniak, and S. Gateva, "Electromagnetically induced transparency and Autler–Townes effect in a generalized Λ-system: a five-level model," Ukr. J. Phys. Opt. **14**, 135–145 (2013).
8. A. Żaba, E. Paul-Kwiek, K. Kowalski, J. Szonert, D. Woźniak, S. Gateva, V. Cao Long, and M. Głódź, "The role of a dipole-coupled but not dipole-probed state in probe absorption with multilevel coupling," Eur. Phys. J. Spec. Top. **222**, 2197–2206 (2013).
9. L. V. Hau, S. E. Harris, Z. Dutton, and C. H. Behroozi, "Light speed reduction to 17 metres per second in an ultracold atomic gas," Nature **397**, 594–598 (1999).
10. D. D. Yavuz, "Electromagnetically induced transparency with broadband laser pulses," Phys. Rev. A **75**, 031801 (2007).
11. C. Liu, Z. Dutton, C. H. Behroozi, and L. V. Hau, "Observation of coherent optical information storage in an atomic medium using halted light pulses," Nature **409**, 490–493 (2001).
12. R. Zhang, S. R. Gardner, and L. V. Hau, "Creation of long-term coherent optical memory via controlled nonlinear interactions in Bose–Einstein condensates," Phys. Rev. Lett. **103**, 233602 (2009).
13. H. Schmid and A. Imamoğlu, "Giant Kerr nonlinearities obtained by electromagnetically induced transparency," Opt. Lett. **21**, 1936–1938 (1996).
14. A. Lambrecht, J. M. Courty, S. Raynaud, and E. Giacobino, "Cold atoms: a new medium for quantum optics," Appl. Phys. B **60**, 129–134 (1995).
15. N. Imoto, H. A. Haus, and Y. Yamamoto, "Quantum nondemolition measurement of the photon number via the optical Kerr effect," Phys. Rev. A **32**, 2287–2292 (1985).
16. W. Leoński and A. Kowalewska-Kudłaszyk, "Quantum scissors—finite-dimensional states engineering," Prog. Opt. **56**, 131–185 (2011).
17. A. Kowalewska-Kudłaszyk, W. Leoński, and J. Peřina, Jr., "Photon-number entangled states generated in Kerr media with optical parametric pumping," Phys. Rev. A **83**, 052326 (2011).
18. A. Kowalewska-Kudłaszyk, W. Leoński, and J. Peřina, Jr., "Generalized Bell states generation in a parametrically excited nonlinear coupler," Phys. Scripta **T147**, 014016 (2012).
19. U. Fano, "Effects of configuration interaction on intensities and phase shifts," Phys. Rev. **124**, 1866–1878 (1961).
20. W. H. Parkinson and E. M. Reeves, "Autoionization resonances and configuration–mixing in the emission spectra of Zn I and Cd I," Proc. R. Soc. London A **331**, 237–247 (1972).
21. K. Rzążewski and J. H. Eberly, "Confluence of bound-free coherences in laser induced autoionization," Phys. Rev. Lett. **47**, 408–412 (1981).
22. G. S. Agarwal, S. L. Haan, and J. Cooper, "Photoemission spectra from autoionizing states under recycling conditions," Phys. Rev. A **28**, 1154–1156 (1983).
23. W. Leoński and R. Tanaś, "DC-field effects on the photoelectron spectrum from a system with two autoionising levels," J. Phys. B **21**, 2835–2844 (1988).
24. A. Raczyński and J. Zaremba, "Threshold effects in photodetachment to a structured continuum," Phys. Rev. A **40**, 1843–1847 (1989).
25. A. Raczyński and J. Zaremba, "Dynamics of a near-threshold photodetachment to a structured continuum," J. Phys. B **23**, 3105–3112 (1990).
26. W. Leoński and V. Bužek, "Quantum laser field effect on the photoelectron spectrum for auto-ionizing systems," J. Mod. Opt. **37**, 1923–1934 (1990).
27. L. Journel, B. Rouvellou, C. Cubaynes, J. M. Bizau, F. J. Wuilleumier, M. Richter, P. Sladeczek, K. H. Selbmann, P. Zimmermann, and H. Bergeron, "First observation of a Fano profile following one step autoionization into a double photoionization continuum," J. Phys. IV **3**, 217–226 (1993).
28. W. Leoński, "Squeezed-state effect on bound-continuum transitions," J. Opt. Soc. Am. B **10**, 244–252 (1993).
29. E. Paspalakis and P. L. Knight, "Population transfer via an autoionizing state with temporally delayed chirped laser pulses," J. Phys. B **31**, 2753–2767 (1998).
30. E. Paspalakis and P. L. Knight, "Restoring dark lines in spontaneous emission via Fano interference," J. Mod. Opt. **46**, 623–631 (1999).
31. M. Lewenstein and K. Rzążewski, "Quantum anti-Zeno effect," Phys. Rev. A **61**, 022105 (2000).
32. A. Zawadzka, R. S. Dygdala, A. Raczyński, J. Zaremba, and J. Kobus, "Three-photon resonances due to autoionizing states in calcium," J. Phys. B **35**, 1801–1817 (2002).
33. W. C. Chu and C. D. Lin, "Theory of ultrafast autoionization dynamics of Fano resonances," Phys. Rev. A **82**, 053415 (2010).
34. J. Zhao and M. Lein, "Probing Fano resonances with ultrashort pulses," New J. Phys. **14**, 065003 (2012).
35. P. R. Sharapova and O. V. Tikhonova, "Dynamics of ionisation and entanglement in the 'atom + quantum electromagnetic field' system," Quantum Electron. **42**, 199–207 (2012).
36. V. Cao Long and M. Trippenbach, "Photoelectron spectra induced by broad-band chaotic light," Z. Phys. B **63**, 267–272 (1986).
37. K. Doan Quoc, V. Cao Long, and W. Leoński, "A broad-band laser-driven double Fano system—photoelectron spectra," Phys. Scripta **86**, 045301 (2012).
38. K. Choudhary, S. Adhikari, A. Biswas, A. Ghosal, and A. K. Bandyopadhyay, "Fano resonance due to discrete breather in nonlinear Klein–Gordon lattice in metamaterials," J. Opt. Soc. Am. B **29**, 2414–2419 (2012).
39. P. Trocha and J. Barnaś, "Quantum interference and Coulomb correlation effects in spin-polarized transport through two coupled quantum dots," Phys. Rev. B **76**, 165432 (2007).
40. A. Ridolfo, O. D. Stefano, N. Fina, R. Saija, and S. Savasta, "Quantum plasmonics with quantum dot-metal nanoparticle molecules: influence of the Fano effect on photon statistics," Phys. Rev. Lett. **105**, 263601 (2010).
41. I. E. Dotan and J. Scheuer, "Fano resonances in vertically and horizontally coupled micro-resonators," Opt. Commun. **285**, 3475–3482 (2012).
42. I. Bayal, B. K. Dutta, P. Panchadhyayee, and P. K. Mahapatra, "Optical analogue of double Fano resonance via dressed twin continua," J. Opt. Soc. Am. B **30**, 3202–3209 (2013).
43. B. Luk'yanchuk, N. I. Zheludev, S. A. Maier, N. J. Halas, P. Nordlander, H. Giessen, and C. T. Chong, "The Fano resonance in plasmonic nanostructures and metamaterials," Nat. Mater. **9**, 707–715 (2010).
44. A. E. Miroshnichenko, S. Flach, and Y. S. Kivshar, "Fano resonances in nanoscale structures," Rev. Mod. Phys. **82**, 2257–2298 (2010).
45. E. Paspalakis, M. Protopapas, and P. L. Knight, "Time-dependent pulse and frequency effects in population trapping via the continuum," J. Phys. B **31**, 775–794 (1998).
46. E. Paspalakis, N. J. Kylstra, and P. L. Knight, "Propagation dynamics in an autoionization medium," Phys. Rev. A **60**, 642–647 (1999).
47. T. Bui Dinh, K. Doan Quoc, V. Cao Long, and K. Dinh Xuan, "Pulse propagation in an autoionization medium with double Fano profile," Eur. Phys. J. Spec. Top. **222**, 2233–2239 (2013).
48. A. Raczyński, M. Rzepecka, J. Zaremba, and S. Zielińska-Kaniasty, "Electromagnetically induced transparency and light slowdown for Λ-like systems with a structured continuum," Opt. Commun. **266**, 552–557 (2006).

49. K. Doan Quoc, V. Cao Long, and W. Leoński, "Electromagnetically induced transparency for $\Lambda$-like systems with a structured continuum and broad-band coupling laser," Phys. Scripta **T147**, 014008 (2012).
50. W. Leoński, R. Tanaś, and S. Kielich, "Laser-induced autoionization from a double Fano system," J. Opt. Soc. Am. B **4**, 72–77 (1987).
51. T. Bui Dinh, V. Cao Long, W. Leoński, and J. Peřina, Jr., "Electromagnetically induced transparency for a double Fano-profile system," Eur. Phys. J. D **68**, 150 (2014).
52. J. Peřina, Jr., A. Lukš, W. Leoński, and V. Peřinová, "Photoionization electron spectra in a system interacting with a neighboring atom," Phys. Rev. A **83**, 053416 (2011).
53. J. Peřina, Jr., A. Lukš, W. Leoński, and V. Peřinová, "Photoelectron spectra in an autoionization system interacting with a neighboring atom," Phys. Rev. A **83**, 053430 (2011).
54. T. Bui Dinh, W. Leoński, V. Cao Long, and J. Peřina, Jr., "Electromagnetically induced transparency in systems with degenerate autoionizing levels in $\Lambda$-configuration," Opt. Appl. **43**, 471–484 (2013).
55. K. Doan Quoc, V. Cao Long, L. Chu Van, and P. Huynh Vinh, "Electromagnetically induced transparency for $\Lambda$-like systems with degenerate autoionizing levels and a broadband coupling laser," Opt. Appl. **46**, 93–102 (2016).